# UNUSUAL CORONAL ACTIVITY FOLLOWING THE FLARE OF 6 NOVEMBER 1980

Z. ŠVESTKA[1], B. R. DENNIS[2], M. PICK[3], A. RAOULT[3], C. G. RAPLEY[4], R. T. STEWART[5], and B. E. WOODGATE[2]

(Received 26 October, 1981)

**Abstract.** For almost 30 hr after the major (gamma-ray) two-ribbon flare on 6 November 1980, 03:30 UT, the Hard X-Ray Imaging Spectrometer (HXIS) aboard the SMM satellite imaged in > 3.5 keV X-rays a gigantic arch extending above the active region over the limb. Like a similar configuration on 22 May 1980, this arch formed the lowest part of a stationary post-flare radio noise storm recorded at metric wavelengths at Nançay and Culgoora. 6.5 hr after the flare a coronal region below the arch started quasi-periodic pulsations in X-ray brightness, observed by several SMM instruments. These brightness variations had no response in the chromosphere (Hα), very little in the transition layer (O v), but they clearly correlated with similar variations in brightness at 169 MHz. There were 13 pulses of this kind, with apparent periodicity of about 20 min, until another flare occurred in the active region at ~ 15:00 UT. All the brightenings appeared within a localized area of about 30000 km$^2$ in the northern part of the active region, but they definitely did not occur all at the same place.

The top of the X-ray arch, at an altitude of ~ 155000 km, was continuously and smoothly decaying, taking no part in the striking variations below it. Therefore, the area variable in brightness does not seem to be the footpoint of the arch, as we supposed for similar variations on 22 May. More likely, it is a separate region connected directly with the source of the radio storm; particles accelerated in the storm may be dumped into the low corona and cause the X-ray enhancements. The X-ray arch was enhanced by two orders of magnitude in 3.5–5.5 keV X-ray counts and the temperature increased from $\lesssim 7.3 \times 10^6$ to $9 \times 10^6$ K when the new two-ribbon flare occurred at 15:00 UT. Thus, it is possible that energy is brought into the arch via the upper parts of the reconnecting flare loops – a process that can continue for hours.

## 1. The Flare

At 03:29 UT on 6 November 1980 a major two-ribbon flare occurred in the active region No. 2779 (NOAA designation), close to the eastern limb (position S 12, E 74). It was an extraordinary event in gamma- and X-rays (class X9 of the NRL scale) and it produced one of the most extensive type IV radio bursts ever observed at Culgoora. Table I gives more details about the flare.

The pointed instruments on Solar Maximum Mission were not observing AR 2779 when the flare occurred (the two experiments mentioned in Table I (HXRBS and GRE) integrate the radiation of the whole solar disk). However, as soon as the flare occurrence had become known, the first opportunity to change the pointing of the satellite was used and the post-flare situation was observed from 06:20 UT. After that the pointed instruments stayed on the active region for several days.

[1] Space Research Laboratory of the Astronomical Institute at Utrecht, The Netherlands.
[2] NASA Goddard Space Flight Center, Greenbelt, Maryland, U.S.A.
[3] Observatoire de Meudon, Meudon, France.
[4] Mullard Space Science Laboratory, University College London, Holmbury St. Mary, Dorking, U.K.
[5] CSIRO, Division of Radiophysics, Culgoora, Australia.

*Solar Physics* **80** (1982) 143–159. 0038–0938/82/0801–0143$02.55.

TABLE I

Characteristics of the flare

| Kind of data | Event | (note) | Beg. | Max. | End | Importance |
|---|---|---|---|---|---|---|
| Hα | flare | (1) | 03:40 | 03:48 | 05:28 | 2 B |
| 1–8 Å X-rays | flare | (1) | 03:29 | 03:52 | 05:33 | X 9.0 |
| > 28 keV X-rays | burst | (2) | 03:24 | 03:48 | | $7.4 \times 10^5$ counts |
| > 300 keV gamma-rays | burst | (3) | 03:44 | | | up to 7 MeV |
| 2.2 MeV line | delayed burst | (4) | | | | 10 $cm^{-2}$ |
| radio microwaves | burst | (1) | 03:35 | 03:46 | 04:55 | up to 12000 FU |
| radio decimetric waves | burst | (1) | 03:44 | 03:48 | 04:30 | up to 92000 FU |
| radio metric waves | type II | (1) | 03:46 | | 04:35 | 3 |
| | type IV | (1) | 03:46 | | 05:15 | 3 |

*Notes*:
(1) Data taken from NOAA (*Solar Geophysical Data* Bulletin).
(2) Data from the HXRBS experiment aboard the SMM (Orwig *et al.*, 1980).
(3) Data from the GRE experiment aboard the SMM (Ryan *et al.*, 1980).
(4) Data from the GRE experiment aboard the SMM (courtesy of E. L. Chupp, University of New Hampshire).

## 2. The Post-Flare X-Ray Arch

From 06:20 through 10:00 UT the Hard X-Ray Imaging Spectrometer (HXIS) aboard the SMM (Van Beek *et al.*, 1980) imaged decaying remnants of the flare in the active region and, high above them, a gigantic X-ray structure extending over the solar limb out of the HXIS field of view. Figure 1, in its left part, shows this situation at the extreme end of this development, at 09:53:00 UT $\pm$ $07^m07^s$ (integrated image for 7:07 min*). We had to choose this particular time for an illustration of the arch, because it was the only time interval when HXIS yielded a complete image of its whole (coarse and fine) fields of view. As one can verify in Figure 2, at all the other times the HXIS X-ray flux was > 60 counts $s^{-1}$, when HXIS automatically changed its program to the 'flare mode', imaging with high time resolution only the brightest parts of its fields of view (comprising 40–60% of the total field). Thus, in order to get the true image of the complete X-ray arch above the active region, we had to select the short time period closely preceding 10:00 UT (cf. Figure 2).

As one can see in Figures 2 and 3, striking variations in the X-ray flux began at 10:00 UT, indicating quasi-periodic oscillations with $P \simeq 20$ min. We will talk about these variations in Section 4. They all happened at the bottom of the arch, above the northern part of the active region, without any fluctuations in brightness at the top of the arch. All the time, as Figure 3 clearly shows, the arch brightness was continuously

* Since June 1980, when HXIS lost one of its two microprocessors, the only remaining microprocessor had to record the solar data for half the time of its operations, and transmit them to the Earth for the other half; thus, 07:07 min of integrated data means 14:14 min of observations.

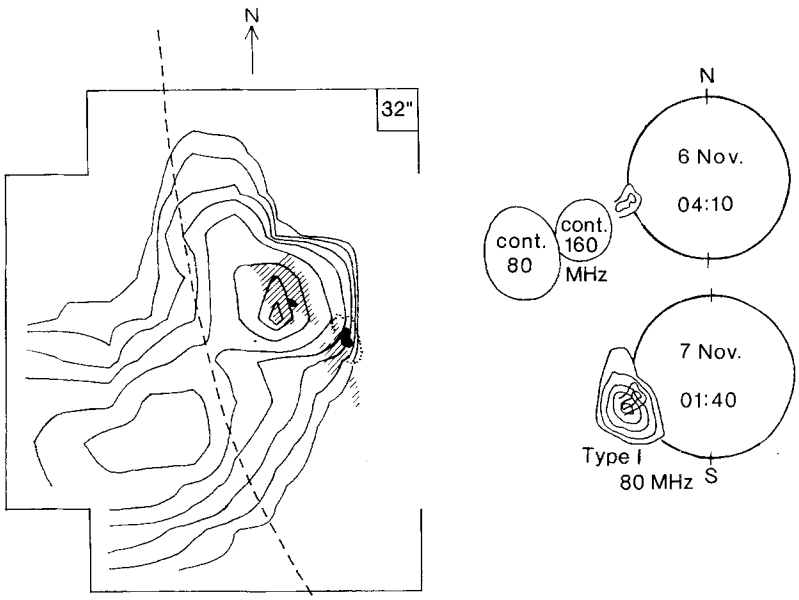


Fig. 1. *Left*: The coronal arch above the active region No. 2779, as imaged by HXIS in 3.5–5.5 keV X-rays with spatial resolution of 32″ at 09 : 53 UT on 6 November 1980 (6.5 hr after the onset of a major two-ribbon flare in the region). The X-ray flux was integrated for 7 min: maximum flux 0.96 counts $s^{-1}$ per element of HXIS coarse field of view (32″ × 32″, the boundaries of the field of view – 6′24″ in diameter – are indicated); the isophote contours are at 90, 75, 50, 25, 12.5, 6.25, 3.12, and 1.06% of the maximum count. The X-ray image is projected on a sketch of the Hα picture of the active region – hatched areas indicate the Hα plage. Two largest spots are also indicated. The dashed line is the solar limb. *Right*: The relative positions of this X-ray arch and images of the stationary type IV radio burst (above) and type I noise storm (below) as seen by Culgoora at 04 : 10 UT on 6 November and 01 : 40 UT next day, respectively. The radio contours are the half-power levels above and 0.7, 0.5, 0.34, 0.24, $0.17 I_{max}$ below.

and smoothly decreasing, until a new flare occurred in the active region at about 14 : 40 UT and caused a new enhancement of the whole arch.

All these characteristics of the arch are reminiscent of the post-flare situation on 22 May, 1980, described earlier by Švestka *et al.* (1982): a gigantic X-ray arch is imaged by HXIS after the occurrence of a major two-ribbon flare, extending along the $H_{\parallel} = 0$ line high into the corona, and recognizable for 8 hr or more in the 3.5–5.5 keV energy range. During this period the brightness at the top of the arch is continuously decaying, whereas striking changes in brightness occur at the bottom of the arch, low in the corona.

The X-ray arch of 22 May was identified by Švestka *et al.* (1982) as the lowest part of a radio noise storm region recorded at Culgoora. The same appears to be the case also on 6 November. Because of night, Culgoora could not observe the Sun when SMM first looked at the east-limb active region: at 10 : 00 UT, when the X-ray contour plot in Figure 1 was obtained, Culgoora's local time was close to midnight. However, both the stationary type IV burst, observed above the flare site before the sunset at Culgoora, and the type I noise storm recorded next morning, were situated in extension of the arch we imaged in X-rays (the right-hand part of Figure 1).

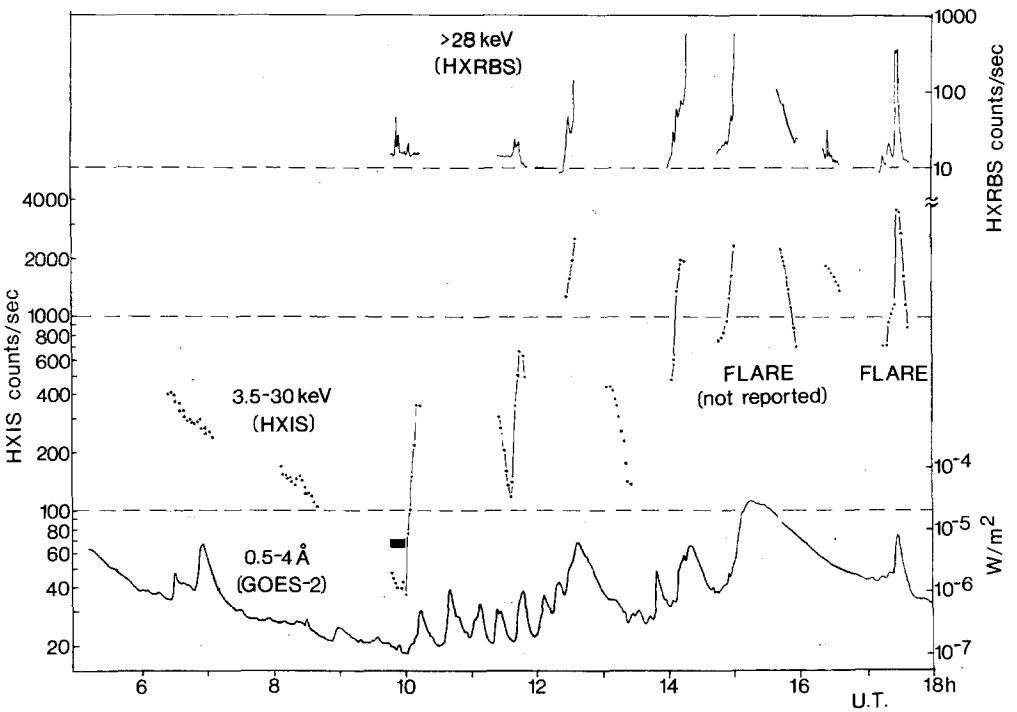


Fig. 2. Time variations of X-rays after the two-ribbon flare that started at 03:30 on 6 November: NOAA–GOES–2 record at 0.5–4.0 Å; SMM records at 3.5–30 keV (HXIS) and > 28 keV (HXRBS). After a continuous decay (the GOES variation at ~ 7 UT came from another region) striking X-ray variations started at 10:00 UT. In spite of the detectability of these variations above 28 keV, no changes could be seen in the high-resolution Ramey Hα pictures of the active region until another flare occurred at about 15:00 UT. The SMM data are interrupted by satellite nights and Southern Atlantic Anomaly effects when the instruments had to be switched off. The bar shortly before 10:00 UT shows the time of the image plotted in Figure 1.

At the time of the SMM observations after 08:50 UT the Sun was under 169 MHz surveillance with the Nançay radioheliograph Mark III. Because of severe ionospheric disturbances the uncertainty in the exact position of the radio source is relatively high ($\sim 0.15 R_\odot$), the more so since two intense type I noise storms in different positions were in progress on the Sun at that time. Nevertheless, one of these sources was definitely above the eastern limb, at about 0.2N and 1.0E in solar radii, and its brightness variations correlated with those observed from 10:00 UT onwards in X-rays. (Cf. Figure 3 and discussion in Section 4.) A similar correlation between brightness at 80 MHz and X-rays was indicated on May 22 (cf. Švestka *et al.*, 1982).

Thus, obviously, the 22 May and 6 November post-flare situations represent similar coronal configurations: *an X-ray-emitting arch-like structure extending high into the corona above a decaying two-ribbon flare site at the bottom of a stationary radio noise storm.* However, the 6 November event was more intense by an order of magnitude as Table II demonstrates. Also Lantos *et al.* (1981) detected a relation between a soft X-ray long-

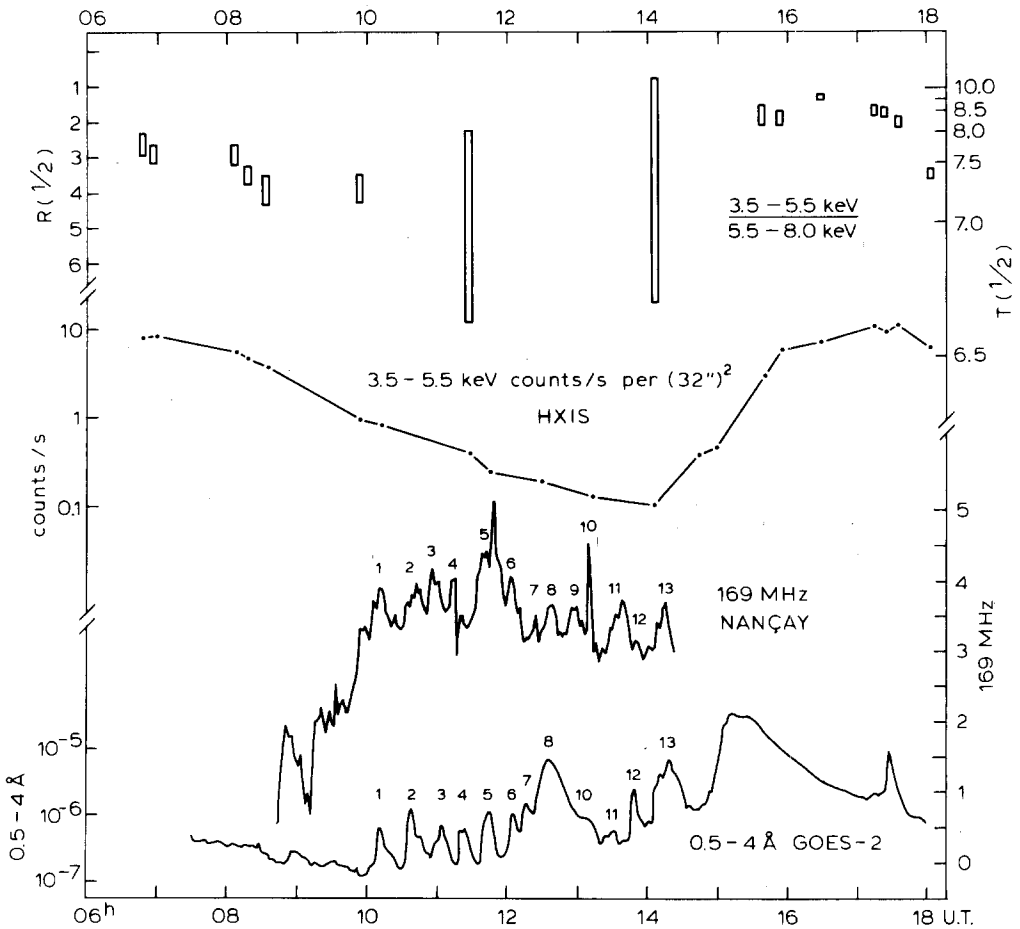


Fig. 3. *Lower part*: The X-ray variations from Figure 2 are compared with Nançay record of type I noise storm at 169 MHz near the eastern solar limb. (1-min integration. Effects of another radio noise storm near the center of the solar disk have been eliminated.) The individual quasi-periodic peaks are numbered 1 through 13 (cf. Table III). *Middle*: Time variation of the maximum intensity at the top of the coronal arch as seen by HXIS in the 3.5–5.5 keV energy range (counts $s^{-1}$ per element of coarse field of view). The flux was continuously decreasing until a new flare appeared in the region shortly before 15 UT. *Upper part*: Time variation of the flux ratio between HXIS energy bands 1 (3.5–5.5 keV) and 2 (5.5–8.0 keV) at the top of the coronal arch (left-hand scale). In case of purely thermal radiation these ratios correspond to the electron temperatures shown in the right-hand scale. (The bars represents $\pm 1\,\sigma$ limits.)

duration event and an intense metric noise storm observed on 30 March, 1980. The storm emission appeared to be located in the northern leg of a loop transient, and this geometry looks similar to the situation described here.

## 3. The Post-Flare Loops

At the beginning of the SMM observations, after 06 : 20 UT, all the pointing instruments (HXIS, UVSP (Woodgate *et al.*, 1980), and FCS (Acton *et al.*, 1980)) imaged 'post-

flare' loops above the active region. Figure 4a shows the tops of the loops in 3.5–5.5 keV X-rays at 06 : 27 UT. The loops were still growing at that time, with a speed of $\sim 2.5$ km $s^{-1}$ between 06 : 27 and 06 : 57 UT, but their X-ray brightness was decaying fast, from a maximum of 6.33 counts $s^{-1}$ per element to 1.58 counts $s^{-1}$ per element of HXIS coarse field of view (32″ × 32″) during the same 30-min time interval. UVSP shows that the decay was fast in the 'hot' Fe XXI line, but O V remained at a high background level.

At 08 : 10 UT, when SMM looked at the flare site in its next orbit, the loop tops were barely visible in 3.5–5.5 keV X-rays and had faded in the Fe XXI line, while the area still remained relatively intense in O V. In X-rays, the plasma in the overlaying arch already became brighter than the loop tops (Figure 4b). The 'post-flare' loops completely disappeared from the X-ray image at about 08 : 20 UT, but instead a new brightening appeared low above the active region (Figure 4c). Both HXIS and UVSP indicate that

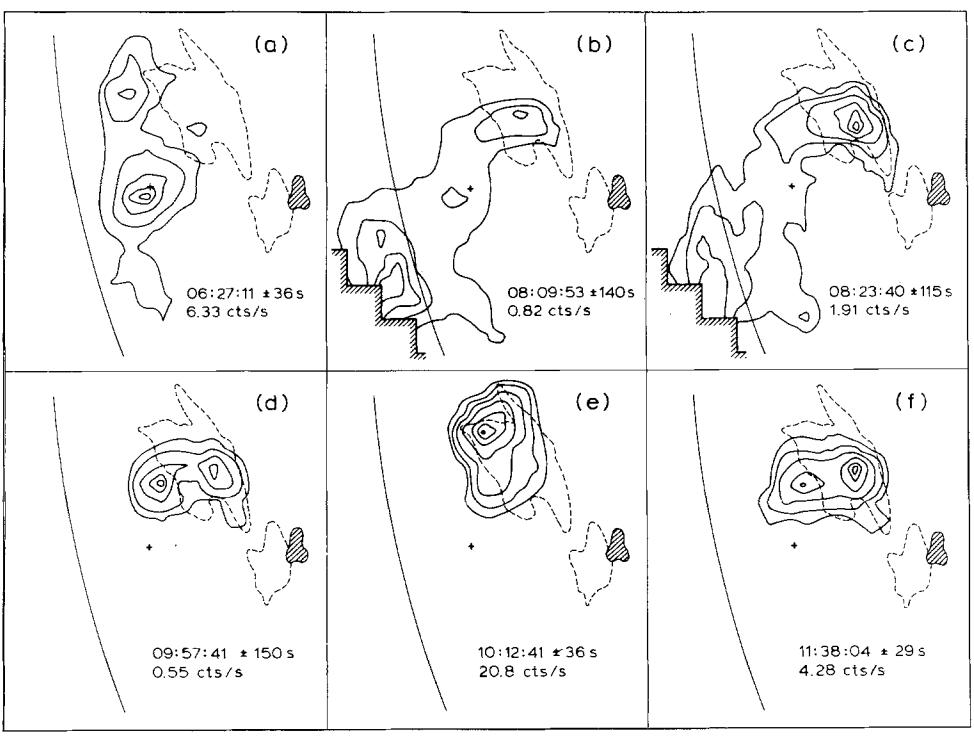


Fig. 4. 3.5–5.5 keV X-ray images of AR 2779 with spatial resolution of 8″ (in the HXIS fine field of view which has 2′40″ in diameter – its boudaries can be seen at 08 : 10 and 08 : 24 UT). The center of the field of view (cross), the solar limb, contours of the Hα plage (dashed lines), and the umbra of the big spot (cf. Figure 1) are indicated. The brightness contours in all X-ray images follow the sequence of 90, 75, 50, 25, 12.5, and 6.25% of the maximum count (c/s given in each frame), except (e), where the contours are at 96, 72, 48, 24, 12, 6, and 3% of max. c/s. The tops of the 'post-flare' loops are clearly imaged in (a); they weaken and eventually disappear in (c), where, however, a new structure forms in the northern part of the active region. All the brightenings in Figures 2 and 3 occurred close to this new structure (like (e)), but the structure remains permanently present (cf. (d) and (f)).

TABLE II

A comparison between the 22 May and 6 November, 1980, X-ray arches

| Date (1980) | 22 May | 6 November |
|---|---|---|
| Flare onset at $t_0$ = | 20 : 50 (21st) | 03 : 30 |
| Max. counts $s^{-1}$ per coarse element of HXIS ($(32'')^2$) in the arch: | | |
| At $t - t_0 = 6.5$ hr: 3.5– 5.5 keV | 0.073 | 0.96 |
| 5.5– 8.0 keV | 0.009 | 0.24 |
| 8.0–11.0 keV | none | 0.033 |
| At $t - t_0 = 9.8$ hr: 3.5– 5.5 keV | 0.033 | 0.13 |
| Last recognizable in X-rays at $t - t_0$ = | $10^h20^m$ | $29^h00^m$ |
| after flare-induced re-enhancement at $t - t_0$ = | – | $11^h15^m$ |
| Max. count $s^{-1}$ per coarse element of HXIS ($(32'')^2$) at the bottom of the arch: | | |
| 3.5– 5.5 keV | 0.110 | 80.0 |
| 5.5– 8.0 keV | 0.020 | 40.0 |
| 8.0–11.0 keV | 0.007 | 8.0 |
| 11.0–16.0 keV | none | 2.0 |
| Variations in X-rays brightness at bottom correlate with radio at: | 80 MHz (Culgoora) | 169 MHz (Meudon) |
| Temperature from 3.5–5.5/5.5–8.0 keV flux ratio at $\Delta t = 6.5$ hr, in $10^6$ K: | 6.2–7.0 | 7.2–7.4 |
| Projected distance of the highest part (top) of the arch (km) | 95000 | 145000 |
| Estimated real altitude (km) | 110000–180000 | ~ 155000 |

this brightening occurred at about 08 : 20, and it was particularly strong in O V. This area then extended to the east and stayed bright, with two distinct maxima (Figure 4d), until the first brightness variation, starting in the active region at 10 : 00 UT and located some 25″ (~ 18000 km) to the north, overpowered it (Figure 4e). But the same area, with the same two X-ray maxima, reappeared again after the brightening declined; and it formed the basic X-ray structure in the active region through all the time of the brightness variations shown in Figures 2 and 3 as we will discuss more in detail in the next section. All these HXIS observations have been confirmed by the UVSP and FCS data; we present here the HXIS images, because one can relate them easily to the X-ray arch which the other experiments could not see because of smaller fields of view.

## 4. The Post-Flare Coronal Brightness Variations

The strange, quasi-periodic variations in X-rays started at 10 : 00 UT (Figure 2). They were seen by the NOAA–GOES-2 experiment in the energy range of 0.5–4.0 Å, by HXIS at > 3.5 keV, and by HXRBS above 28 keV. The amplitude of these variations was much smaller in the 1–8 Å GOES-2 channel. Hence these variations were most pronounced below 4 Å (i.e. above 3 keV).

Because of the satellite nights and unfavourably located South Atlantic Anomalies (when the SMM instruments had to switch off) the HXIS and HXRBS could see only

a few of these pulsating X-ray enhancements (cf. Figure 2). Nevertheless, even the greatly interrupted observations clearly indicate that the subsequent X-ray peaks were progressively more intense and harder in their energy spectrum.

### 4.1. Correlation with 169 MHz Noise Storm

On 22 May, 1980, we saw similar X-ray variations at the supposed 'western footpoint' of the post-flare coronal arch which seemed to correlate with brightness-temperature variations at 80 MHz high in the corona in the radio noise storm region (Švestka *et al.*, 1982). A similar effect is seen here as well. As Figure 3 (bottom) shows, the radio noise storm above the eastern solar limb, observed at Nançay at 169 MHz, appears to show variations in radio brightness very similar to those observed in X-rays.

The general rise at the metric radio waves starts before 09:00 UT and may be associated with the formation of the newly brightened area which was first seen in X-rays at 08:20 (cf. Section 3). The first radio flux variation might coincide with a small X-ray peak at 08:54; but clear variations are seen in X-rays only from 10:00 UT onwards. We have numbered these variation peaks from 1 through 13 in Figure 3, and 9 of them seem to occur at the same time both in the X-rays and at 169 MHz. A detailed comparison is shown in Table III.

TABLE II

The brightness peaks between 10:00 and 14:20 UT

| Peak No. | Time | | Time difference X-rays – radio | Time interval between peaks | |
|---|---|---|---|---|---|
| | in X-rays | at 169 MHz | | in X-rays | at 169 MHz |
| 1 | 10:12 | 10:10 | +2 min | 29 min | |
| 2 | 10:41 | 10:39 | +2 min | 24 min | 29 min |
| 3 | 11:05 | 10:57 | +8 min | 17 min | 18 min |
| 4 | 11:22 | ? | | 24 min | |
| 5 | 11:46 | 11:45 | +1 min | 20 min | |
| 6 | 12:06 | 12:05 | +1 min | 14 min | 20 min |
| 7 | 12:20 | 12:25 | −5 min | 18 min | 20 min |
| 8 | 12:38 | 12:37 | +1 min | | 12 min |
| 9 | – | 12:57 | | | 20 min |
| 10 | 13:11 | 13:12 | −1 min | 21 min | 15 min |
| 11 | 13:32 | 13:36 | −4 min | 16 min | 24 min |
| 12 | 13:48 | 13:51 | −3 min | 31 min | 15 min |
| 13 | 14:19 | 14:12 | +7 min | | 21 min |
| Mean | | | $+00^m48^s$ | $21^m24^s$ | $19^m24^s$ |
| Standard deviation | | | $\pm\ 3^m34^s$ | $\pm\ 5^m35^s$ | $\pm\ 4^m51^s$ |

It was possible to separate the 169 MHz radiation coming from a position near the eastern limb from a region near the Sun's center which was the source of another radio noise storm during the studied period. This central region does not show any of the semi-periodic variations between 10:00 and 14:00 UT so that the reality of these radio

changes and their origin in the AR 2779 are well established. On the other hand, the general flux increase observed by GOES after ~ 12 : 00 UT is better associated with the radio flux from the region near the disc center.

### 4.2. Absence of chromospheric excitation

In spite of the fact that the X-ray brightenings between 10 : 00 and 14 : 00 UT resemble flares, with HXRBS recording the individual variations above 28 keV in all the peaks that occurred during the SMM 'days', no changes at all could be detected in the chromosphere for any of these X-ray enhancements. By the courtesy of the SMY coordinator, D. M. Rust, we have had at our disposal a complete Ramey sequence of high-resolution Hα images of the AR 2779 from 11 : 09 onwards. Apart from looking at the pictures ourselves, we have shown these high-quality Hα images to several experienced observers, including H. W. Dodson-Prince, E. R. Hedeman, and D. M. Rust; none of them could detect any slightest flare-like change in the active region below the X-ray brightenings. Thus one can conclude that the variations were purely coronal phenomena, without any detectable impact upon the chromosphere.

The only Hα change seen during this period (from 10 : 00 through 14 : 00 UT) was a surge, repeatedly emerging from the penumbra of the large spot shown in Figure 1, and a bright point appearing in the spot penumbra at the footpoint of this surge. At least some peaks of the X-ray variations (cf. the example at 11 : 40 in Section 4.5) seem to be synchronized with the surge reappearance. But this location was quite far from the site where the X-ray brightenings occurred.

The first change in Hα which occurred close to the position of the X-ray brightenings could be seen after 14 : 00 UT (peak No. 13 in Figure 3): the off-band Hα pictures showed a tiny dash-like enhancement in the penumbra of the other spot, close to the maximum X-ray flux in Figure 1. But only at 14 : 50 did the first real flare occur. Ramey still did not classify it as a flare (and no other Hα-patrol station did either), but it was clearly an anomalously faint two-ribbon flare. (E. R. Hedeman said she would classify it as 2F in Hα, a rather unusual classification). After that, at 17 : 26, another flare occurred, duly reported by the patrol stations.

### 4.3. Brightness and Temperature of the X-ray arch

In the middle part of Figure 3 we show the maximum counts $s^{-1}$ per HXIS coarse element in the X-ray arch as a function of time. One can see that the X-ray arch brightness (i.e. the maximum above the limb in Figure 1) was decreasing continuously and smoothly all the time, completely ignoring the X-ray and radio variations that started at 10 : 00 UT. Only shortly before 15 : 00 UT, when the faint two-ribbon flare occurred in the active region, did the brightness of the X-ray arch become enhanced again. Similar enhancements of the arch brightness followed some other flares on the next few days (as we will discuss in another paper). But nothing like that happened during the X-ray variations prior to 14 : 00 UT, which is another evidence that these variations represent a phenomenon distinctly different from flares.

The same behavior of the X-ray arch was seen on 22 May, 1980: whereas there were strong variations in X-ray brightness below the arch (at a supposed 'footpoint'), the top of the arch was decaying smoothly and did not reflect any of these variations. Also no Hα brightenings were recorded at those times.

The upper part of Figure 3 shows the 3.5–5.5 keV/5.5–8.0 keV flux ratio at the top of the arch. If we assume that this radiation was from a thermal plasma, the arch temperature was $7.7 \times 10^6$ K at 06:45 UT (three hours after the flare maximum), decreasing slightly to $\sim 7.3 \times 10^6$ K three hours later. For several more hours the flux was too low to allow a reliable estimate of $T$ without a very long integration (cf. the $\pm 1\sigma$ limits plotted in Figure 3). Only after the new arch enhancement, from 15:00 UT onwards, could temperature values be obtained again. They show a temperature increase up to $9 \times 10^6$ K. In comparison, the temperature at the top of the arch of 22 May was found to be rather constant and close to $6.5 \times 10^6$ K, hence somewhat cooler than we have found in this case.

### 4.4. Location of the brightenings

The HXIS coarse field of view images show that the brightenings after 10:00 UT occurred in the northern part of the active region, close to the northern spot, and that their positions were shifted slightly to the N and NW of the original maximum of X-ray brightness, shown in Figure 1. However, we cannot determine for sure from the coarse field image whether all the brightenings occurred at the same place or whether different locations in the active region were involved. We encountered the same difficulty of low spatial resolution in the 22 May event. Fortunately, this time the brightenings occurred inside the fine field of view of HXIS, as well as in the fields of view of the UVSP and FCS instruments. Therefore, much better information on the location of the individual brightenings can be obtained for this event.

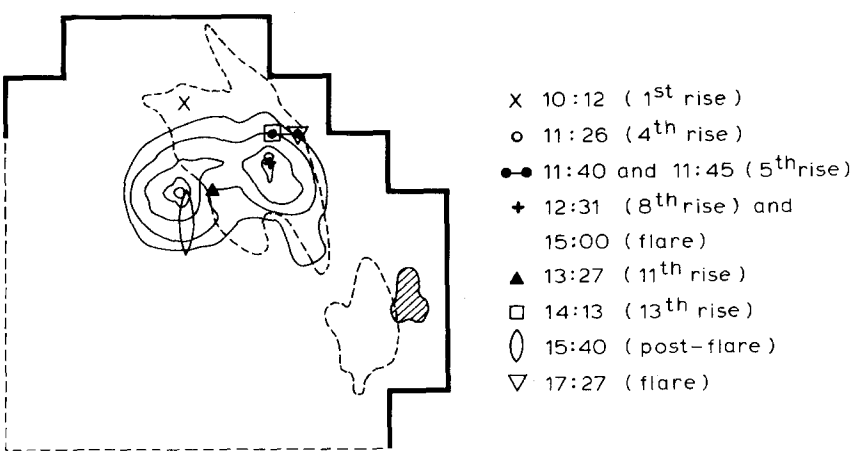


Fig. 5. Positions of the individual X-ray brightenings starting at 10:00 UT (cf. Figure 3 for their numbering) compared with the X-ray contours at 09:57 UT (taken from Figure 4d). [Kindly correct 13:27 (11th rise) to 13:08 (10th rise)].

The fine field of view of HXIS, with the brightness distribution in 3.5–5.5 keV X-rays taken from Figure 4d (09 : 57 UT), is shown in Figure 5. Over that background we have plotted the position of maximum brightness for the brightenings Nos. 1, 4, 5, 8, 10, and 13, as well as for the flares at 15 : 00 and 17 : 27 UT. All the brightenings 1–13, as far as HXIS could see them, were narrowly localized phenomena, with intensity exceeding 30% of the maximum counts in no more than four 8″ × 8″ HXIS pixels. More than 50% of the maximum flux was usually seen in one pixel only. That means that most of the X-ray enhancements were restricted to an area smaller than 10 000 km and possibly less than 5000 km in diameter.

As Figure 5 shows, all the brightenings (which SMM could image) occurred close to the area that newly brightened at 08 : 20 UT (cf. Section 3 and Figure 4). The brightenings are scattered throughout an area of about $(30\,000\ \text{km})^2$ (in projection); as a matter of fact, four of the brightenings seen by the SMM, plus the original sites of both the flares occurred within an area of $(10\,000\ \text{km})^2$. Only the 1st and 10th peaks were at different locations. (The 15 : 40 UT image probably shows the tops of post-flare loops after the flare of 15 : 00 UT.)

We can thus conclude that the brightenings 1–13 were confined to a relatively small area in the northern part of the AR 2779. However, they definitely did not occur all at the same place. Therefore, the suggested periodicity of the enhancements in Figures 2 and 3 and Table III does not mean brightness pulsations at one definite place on the Sun. Slightly different small areas brightened every time. Within the spatial resolution of the HXIS fine field of view, some occurred at the same place, e.g. the peaks Nos. 4 and 8, or 5 and 13, but others in between occurred elsewhere.

### 4.5. Details of the brightenings nos. 1 and 5

Figure 6 shows the details of the brightening No. 1 starting at 10 : 00 UT on 6 November. Two records by HXIS are in the middle part of the figure: the record marked 'A.R.' is the 3.5–5.5 keV flux in the brightest element of HXIS coarse field of view (32″ × 32″) above the active region (cf. the maximum flux projected on the solar disk in Figure 1); the other, in the same energy range, is the brightest element of HXIS coarse field of view in the X-ray arch (cf. the maximum just above the limb in Figure 1). Evidently, the enhancement was confined completely to the low coronal layers, above the active region; the arch itself, as also Figure 3 has shown, did not participate at all in the brightenings.

Above the HXIS records we plot the Fe XXI brightness in a smaller area (10″ × 10″) centered at the brightest point within the region of the HXIS 'A.R.' flux. Obviously, the behavior in the Fe XXI line was about the same as in the 3.5–5.5 keV X-rays and peaked at the same time as the HXIS flux. This is not surprising since Fe XXI corresponds to a temperature $T \simeq 12 \times 10^6$ K, close to the temperature expected in the X-ray source (at 10 : 12 : 16 UT the 3.5–5.5/5.5–8.5 keV flux ratio of the brightest element in HXIS coarse field of view corresponded to $T = 7.4 \times 10^6$ K, and the 3.5–5.5/8.5–11.0 keV ratio to $T = 12.5 \times 10^6$ K).

On the other hand, the lowest curve represents the record of the same 10″ × 10″

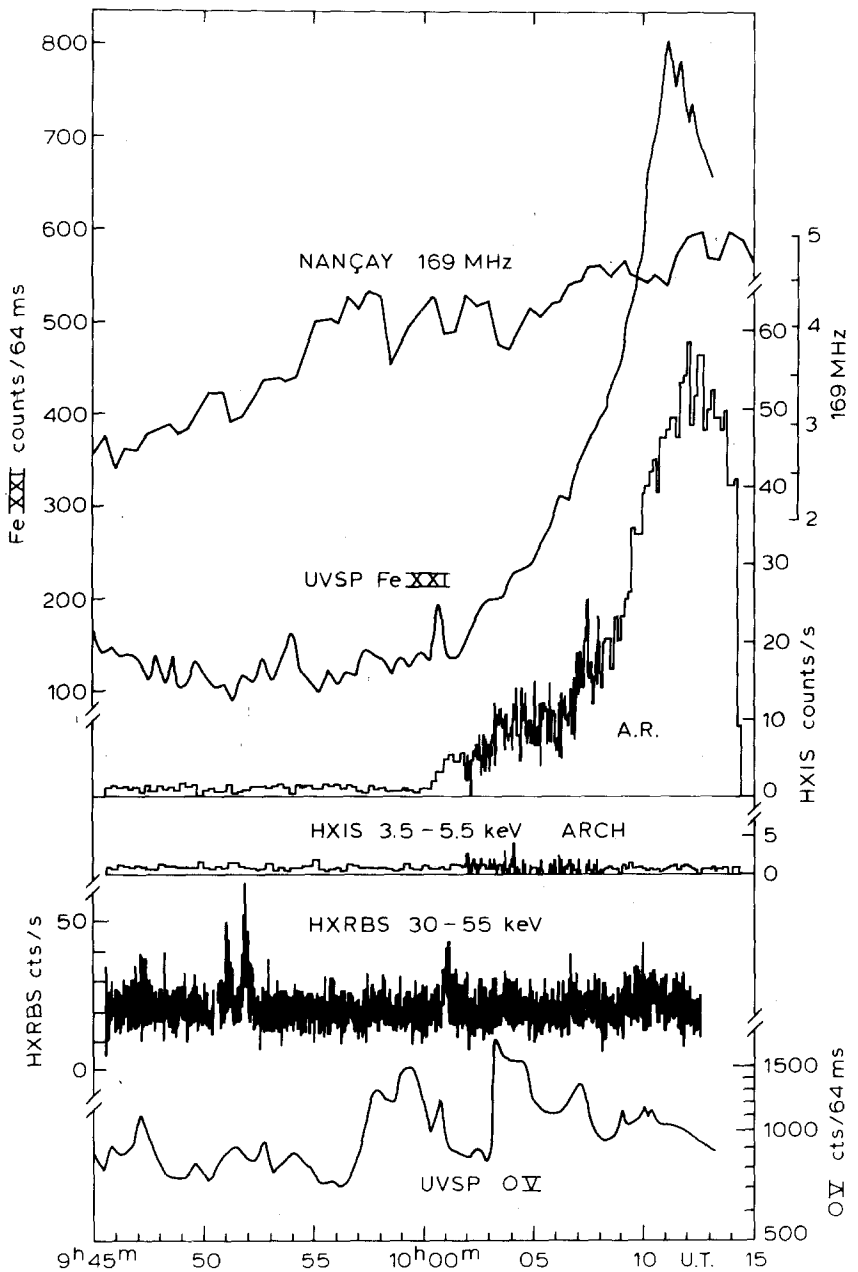


Fig. 6. Details of the first brightening at 10 : 00 UT. *From below*: flux variations in the O v line of the UVSP experiment: the brightest 10″ × 10″ pixel within a 180″-squared area centered at the position of the brightening shown in Figure 5; 30–55 keV hard X-ray flux, integrated over the solar disk (HXRBS); 3.5–5.5 counts $s^{-1}$ in the brightest 32″-squared element in the coronal arch above the active region (HXIS); 3.5–5.5 keV counts $s^{-1}$ within a 32″-squared element at the position of the brightening shown in Figure 5 (HXIS); Fe XXI flux of the brightest 10″ × 10″ pixel in the same 180″ × 180″ area as O v (UVSP); record at 169 MHz of the radio noise storm near the eastern solar limb (Nançay; arbitrary linear scale, integration time 30 s).

region in the O V line corresponding to $T \simeq 2.5 \times 10^5$ K in the transition layer. While there are some uncorrelated small variations in the O V flux (by about a factor of 2) starting at $\sim 09:56$ UT, there is no enhancement at all at the time of X-ray and Fe XXI flux increase. Thus the transition layer did not participate in the enhancement after 10:08 UT, and the rise was clearly a purely coronal matter.

The > 30 keV X-rays show only very small enhancements during this period. The peaks at 09:51 and 09:52 UT might have come from another region on the Sun, since no evidence for an X-ray enhancement can be seen within the fields of view of the pointed instruments aboard the SMM. However, the peak at 10:01 UT seems to be associated with the discussed enhancement, because it coincides with the onset of HXIS brightening and has some response in the O V and Fe XXI data.

Figure 7 shows similar records for the brightening No. 5, preceded by the decay of the rise No. 4. In > 30 keV X-rays we see a behavior similar to that for peak No. 1, but much more clearly defined: a hard X-ray peak at the onset of the increase in brightness at softer energies. Thus, both the brightenings Nos. 1 and 5 are consistent with the commonly observed flare behavior in X-rays: an enhancement in soft X-rays with a short-lived hard X-ray burst near the onset. This hard X-ray burst is also reflected in the transition layer (O V); but after that the transition layer does not seem to be affected by the rise, and neither is the chromosphere (H$\alpha$) as we mentioned earlier (Section 4.2).

The chromosphere, however, showed a brightening at the footpoint of a surge in the penumbra of the big spot at the time of the hard X-ray burst and O V enhancement (cf. Section 4.2). This area was far from the region of the X-ray and Fe XXI brightening, and no increase in flux was seen by HXIS in that position. The O V line, however, brightened at 11:40 UT at both locations: where the X-rays brightened, as well as where the H$\alpha$ bright point appeared.

The second peak at > 30 keV in Figure 7 coincides with the brightenings in > 3.5 keV X-rays and Fe XXI. However, as HXIS shows clearly in its fine field of view, this second peak of HXRBS occurred at a slightly different place than the original hard X-ray burst (cf. the positions of the two dots in Figure 5; the second peak was more to the west). Like the brightening after 10:08 UT in Figure 6, this second (main) rise had no response in the transition layer (O V) or in H$\alpha$.

The upper curves in Figures 6 and 7 show records of the radio noise storm above the eastern limb at 169 MHz. The radio flux begins to rise some 10–15 min before the onset of the X-ray enhancement and peaks at the same time (Figure 6) or slightly later (Figure 7). Because the individual records in Figure 7, from below upwards, roughly correspond to increasing altitude in the solar atmosphere, an impression could be obtained that the enhancement propagates upwards (with $v \simeq 500$ km s$^{-1}$), following a trigger near the transition layer. However, the facts that the 11:40 UT burst occurred in a different position, and that the delay at 169 MHz is not observed in all the peaks (cf. Table III), argue against this conclusion. The earlier onset at 169 MHz suggest rather that the disturbance has its origin high in the corona.

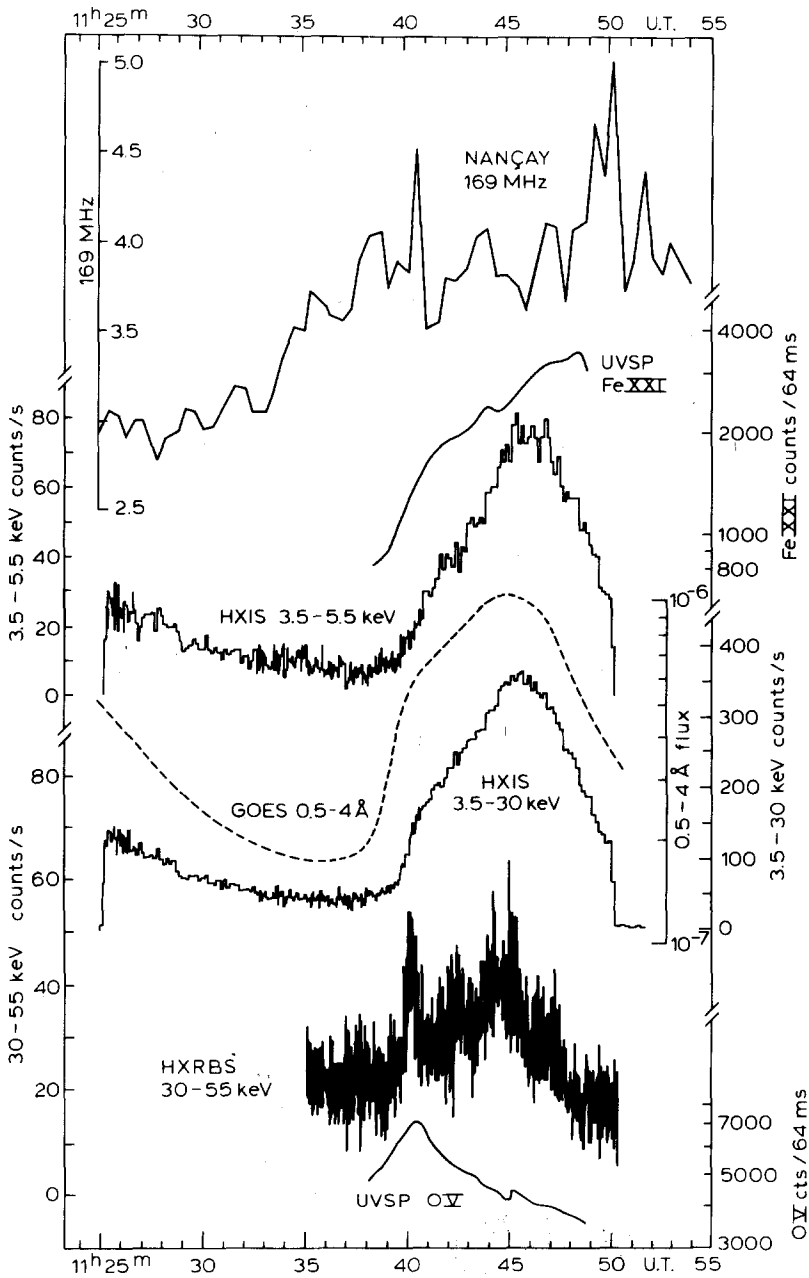


Fig. 7. Details of the fifth rise in brightness (cf. Figure 3 for the numbering). *From below*: Flux in the O v line, for an area of 30″ × 30″ at the position of the brightening shown in Figure 5 (UVSP); > 30 keV X-ray flux, integrated over the solar disk (HXRBS); total flux recorded by HXIS in its fine and coarse fields of view (comparable with the HXIS record in Figure 2); total 0.5–4 Å flux recorded by NOAA–GOES-2 from the whole Sun; 3.5–5.5 keV counts $s^{-1}$ within a 32″-squared element at the position of the brightening shown in Figure 5 (HXIS); Fe XXI flux, same mode as O v (UVSP); record at 169 MHz of the radio noise storm near the eastern solar limb (Nançay; arbitrary linear scale, integration time 30 s).

## 5. Discussion

These observations on 6 November 1980 pose several puzzling problems. First, the relatively low spatial resolution of the SMM instruments does not allow us to understand the nature of the structure that first appeared at about 08 : 20 UT and later became the seat of the X-ray variations. The following information about this structure is available:

(a) It was different from the post-flare loops, because it appeared below them at the time when the loops, much higher up, completely disappeared in X-rays (Figure 4).

(b) The region, when formed, was located low in the corona (> 3.5 keV X-rays and Fe XXI showed it) and in the transition layer (visible in O V); at that time we have no information on changes in the chromosphere.

(c) When the X-ray brightenings occurred (after 10 : 00 UT) inside this area or very close to it (Figure 5), only the corona was affected: no changes could be seen in the H$\alpha$ line and very small changes occurred in the transition layer (O V).

(d) This region had to be connected in some way with the radio noise-storm region high in the corona, because the brightness variations in this area appear to be correlated with variations at 169 MHz (Figures 3, 6, 7 and Table III).

(e) Contrary to that, no correlation in brightness variations can be found between this region and the X-ray arch; still, the X-ray images indicate a connection between this area and higher regions of the solar corona (cf. Figures 1 and 4).

On 22 May, 1980, we saw a similar region fluctuating in brightness below the giant X-ray arch and we supposed that it was one of the arch footpoints. We considered it to be the western footpoint, but it might have been the central one, with the western footpoint out of the HXIS field of view; or, it might have been a region completely detached from the arch (Švestka *et al.*, 1982).

This is true on 6 November as well. The area fluctuating in X-ray brightness might be one of the footpoints of the arch, but then it is really difficult to understand why the top of the arch did not participate in the brightness variations. It seems more likely that it is not the footpoint, but an independent area below the arch, directly connected with the noise-storm region. Then, obviously, we postulate the existence of two gigantic loop-like structures above the post-flare active region: one is the X-ray arch, demonstrated in Figure 1, with maximum X-ray brightness near its top, at about 155 000 km above the photosphere, and with footpoints invisible in X-rays; apparently the maximum X-ray brightness is near the top and decreases steadily downwards. The other structure connects the fluctuating area of Figure 5 with the radio noise-storm region at a supposed altitude of about 250 000 km. A somewhat similar situation was also discussed by Lantos *et al.* (1981) for the 30 March 1980 limb event.

Another problem is the nature of the quasi-periodic brightenings. As in flares, we see soft X-ray enhancements with hard X-ray bursts near their onsets (e.g., Figure 7). However, in all other aspects the brightenings differ from flares. In particular:

(a) There is no flare-like brightening in the chromosphere (H$\alpha$ line) and very little in the transition layer (O V).

(b) The X-ray arch, which is enhanced by flares that occur below it, does not respond to these brightenings.

(c) Still higher in the corona, variations in brightness temperature of a radio noise-storm region correlate with the X-ray brightenings, which is an effect quite different from the radio bursts (of types II, III, IV, or V) commonly associated with flares.

When studying the 22 May 1980 event, we suggested that the brightenings had their origin in the radio noise-storm region (Švestka *et al.*, 1982): this region is a permanent source of intermittent particle acceleration; some of the acceleration processes there are anomalously strong, the accelerated particles penetrate deep into the low corona and produce X-rays in the lowest coronal layers through bremsstrahlung. There is no apparent reason in the 6 November data why we should modify this hypothetical interpretation, but the problem still remains puzzling.

First, the particles propagating downwards must lose their energy before they get through the transition layer to the chromosphere. This would seem reasonable if the corona above the active region were still sufficiently filled with material as an aftermath of the X9 flare. The UVSP O v-line observations support this picture: the background brightness in O v at the time of the X-ray enhancements is about 5000 erg $cm^{-2}$ $s^{-1}$ $sr^{-1}$ in the region where several enhancements occurred according to Figure 5. This is about six times brighter than for the same region two days later. Since the O v-line emission is proportional to density squared, this enhancement is an evidence that there is much more material than normal in the active region transition zone. Hence enhanced density can be expected also in the low corona. Whether there is enough material to stop an electron beam from penetrating through to low-temperature atmosphere would depend on the number and energy spectrum of the dumping electrons.

However, even if this explanation works, there is still another problem: why is heat conduction unable to transport at least some energy from the enhanced corona with temperature in excess of $7 \times 10^6$ K through the transition layer to the H$\alpha$ emitting region? A more detailed study of both these problems is under preparation and we intend to present it in a following paper (Švestka *et al.*, 1983).

Finally, the arch itself poses another puzzle. Without repeating most of the problems mentioned by Švestka *et al.* (1982; the reader is kindly requested to read Section 7 of that paper), we want to emphasize the following two questions:

(a) When and how does the arch originate? Both on 21/22 May and 6 November we saw it first after a major two-ribbon flare. On 21 May its origin seemed to coincide with the formation of a stationary type IV (continuum) burst above the active region that later changed into the type I noise-storm. (We did not see the initial phase on 6 November.) So it is a reasonable conjecture to assume that the arch was formed by a process associated with this flare, possibly as a remnant of the filament disruption at the flare onset. But on 6 November, after the arch had severely decayed, it reappeared again when a new two-ribbon flare occurred in the active region (cf. Figure 3). Thus, as it seems, the arch, once being formed, becomes a rather permanent configuration above the active region. We intend to discuss the whole life story of the 6 November arch and its revivals in another paper.

(b) What is the source of energy for the arch? Švestka *et al.* (1982) suggested two alternatives: (i) If the brightness variations occur at the footpoints of the arch, being

caused by accelerated particles that are dumped into the low corona, some particles may be trapped in the X-ray arch and get thermalized there. Thus, successive particle dumps can feed the arch for many hours with additional energy. (ii) Another source for energy supply might be the reconnection of flare loops below the arch which can continue for many hours. Particles accelerated in the process of reconnection can be trapped in the arch because the upper disconnected loops are interconnected along the $H_{\parallel} = 0$ line (Anzer and Pneuman, 1982).

The fact that new two-ribbon flares revive the arch, whereas variations in the radio region above and in the X-ray region below do not affect the arch, support strongly the second interpretation: *Energy is brought into the arch through the upper parts of the reconnecting flare loops* (cf. Figure 10 in Švestka *et al.*, 1982). This process can continue – with decreasing energy supply – for many hours.

## Acknowledgements

The development and construction of the Hard X-Ray Imaging Spectrometer was made possible by the support given by the Netherland Ministry for Education and Science, through the Committee for Geophysics and Space Research of the Royal Dutch Academy of Arts and Sciences, and the Science Research Council of the United Kingdom. C. G. Rapley acknowledges the support of the UK Science and Engineering Research Council. The Hard X-Ray Burst Spectrometer and the Ultraviolet Spectrometer and Polarimeter and the SMM satellite were provided by NASA.

Our thanks are due to E. L. Chupp for his kind permission to use unpublished gamma-ray data in Table I, D. M. Rust for providing us with high-quality Hα data of the Ramey station, and D. Speich for help in the positional alignment of the HXIS and Hα pictures. We acknowledge instructive discussions on the treated topics with H. W. Dodson-Prince, E. R. Hedeman, H. S. Hudson, D. M. Rust, G. M. Simnett, and B. Somov, and careful preparation of the figures by H. Braun.

## References

Acton, L. W., Culhane, J. L., Gabriel, A. H., and 21 co-authors: 1980, *Solar Phys.* **65**, 53.

Anzer, U. and Pneuman, G. W.: 1982, *Solar Phys.* **79**, 129.

Lantos, P., Kerdraon, A., Rapley, C. G., and Bentley, R. D.: 1981, *Astron. Astrophys.* **101**, 33.

Orwig, L. E., Frost, K. J., and Dennis, B. R.: 1980, *Solar Phys.* **65**, 25.

Ryan, J. M., Chupp, E. L., Forrest, D. J., Reppin, C., Reiger, E., Kambach, G., Pinkau, K., Shore, G., and Krieger, R. L.: 1980, *Bull. Am. Astron. Soc.* **12**, 891.

Švestka, Z., Stewart, R. T., Hoyng, P., Van Tend, W., Acton, L. W., Gabriel, A. H., Rapley, C. G., and 8 co-authors: 1982, *Solar Phys.* **75**, 305.

Švestka, Z., Schrijver, J., Somov, B., Dennis, B. R., Woodgate, B. E., Fürst, E., Hirth, W., Klein, L., and Raoult, A.: 1983, to be submitted to *Solar Phys.*

Van Beek, H. F., Hoyng, P., Lafleur, H., and Simnett, G. M.: 1980, *Solar Phys.* **65**, 39

Woodgate, B. E., Tandberg-Hanssen, E. A., Bruner, E. C., and 11 co-authors: 1980, *Solar Phys.* **65**, 73.